water

MDPI

Article

Quantitative Analysis of Droplet Size Distribution in Plant Protection Spray Based on Machine Learning Method

Yong He [1], Jianjian Wu [1], Haoluan Fu [1], Zeyu Sun [2], Hui Fang [1,3,*] and Wei Wang [1]

[1] College of Biosystems Engineering and Food Science, Zhejiang University, Hangzhou 310058, China; yhe@zju.edu.cn (Y.H.); 11713011@zju.edu.cn (J.W.); 3160100471@zju.edu.cn (H.F.); wwang_2017@zju.edu.cn (W.W.)
[2] Synergistic Innovation Center of Jiangsu Modern Agricultural Equipment and Technology, Jiangsu University, Zhenjiang 212013, China; 1000004203@ujs.edu.cn
[3] Digital Village Laboratory, Huzhou Institute of Zhejiang University, Huzhou 313099, China
* Correspondence: hfang@zju.edu.cn

Abstract: Spray droplet size is the main factor affecting the deposition uniformity on a target crop. Studying the influence of multiple factors on the droplet size distribution as well as the evaluation method is of great significance for improving the utilization of pesticides. In this paper, volume median diameter (VMD) and relative span (RS) were selected to evaluate the droplet size distribution under different hollow cone nozzles, flow rates and spatial positions, and the quantitative models of VMD and RS were established based on machine learning methods. The results showed that support vector regression (SVR) had excellent results for VMD (R_c = 0.9974, R_p = 0.9929), while multi-layer perceptron (MLP) had the best effect for RS (R_c = 0.9504, R_p = 0.9537). The correlation coefficient of the prediction set is higher than 0.95, showing the excellent ability of machine learning on predicting the droplet size distribution. In addition, the visualization images of the droplet size distribution were obtained based on the optimal models, which provided intuitive guidance for realizing the uniform distribution of pesticide deposition. In conclusion, this study provides a novel and feasible method for quantitative evaluation of droplet size distribution and offers a theoretical basis for further determining appropriate operation parameters according to the optimal droplet size.

Keywords: droplet size distribution; machine learning; plant protection spray; quantitative model

check for updates

Citation: He, Y.; Wu, J.; Fu, H.; Sun, Z.; Fang, H.; Wang, W. Quantitative Analysis of Droplet Size Distribution in Plant Protection Spray Based on Machine Learning Method. *Water* **2022**, *14*, 175. https://doi.org/10.3390/w14020175

Academic Editor: Pilar Montesinos

Received: 29 October 2021
Accepted: 7 January 2022
Published: 9 January 2022

Publisher's Note: MDPI stays neutral with regard to jurisdictional claims in published maps and institutional affiliations.

Copyright: © 2022 by the authors. Licensee MDPI, Basel, Switzerland. This article is an open access article distributed under the terms and conditions of the Creative Commons Attribution (CC BY) license (https://creativecommons.org/licenses/by/4.0/).

1. Introduction

Plant protection spray has been widely used to prevent and control diseases and pests due to its high efficiency, rapidity and economy. It plays an irreplaceable role in ensuring food security [1]. During the spraying process, a fraction of pesticides are lost in the air due to the droplet drift [2]. In addition, pesticides also exist in the soil on account of the run-off and rebound of droplets. The volatilization and wind erosion of soil particles will increase the pesticide content in the atmosphere, which causes air pollution and poses a threat to human health and safety [3,4]. The imperfect plant protection spraying technology not only leads to the low utilization rate of pesticides, but also seriously endangers the agricultural product safety and the environment [5]. With the increasing awareness of global environmental protection, how to maximize the effectiveness of pesticides has attracted widespread attention. It is necessary to improve pesticide utilization and reduce human exposure to atmospheric pesticides [4].

Studies have found that it is necessary to ensure the uniformity of pesticide spray coverage for maximum efficacy [6,7]. The droplet size of pesticides is the main factor that directly affects the distribution uniformity on the target crop [8]. In the spray process, large droplets are not easy to drift or evaporate but are likely to bounce or roll off. As a result, liquid loss, pollution of soil and water, as well as poor coverage density and uniformity of droplets can occur, which greatly reduces the effectiveness of pesticide

spray effect [9]. On the contrary, the small droplets have excellent adhesion, coverage density and uniformity on the crop surface. However, they are prone to drift, which causes environmental pollution as well as damage to other crops nearby [10–13]. According to the theory of Biological Optimum Droplet Size (BODS), the range of droplet size captured by different biological targets is different. Only droplets within the optimal size range are effective for specific target organisms [14–16]. Therefore, reasonable droplet size is key to achieve the best prevention and control effect with the least amount of pesticides and to reduce environmental pollution. In order to achieve the expected prevention and control effect, appropriate pesticides should be sprayed to the target crops to obtain optimal droplet coverage density [6,17]. This conclusion negates the possibility of blindly increasing the dosage to improve the prevention and control effect. Washington [18] indicated that the linkage change of the spray coverage density can be realized by controlling the volume median diameter (VMD) of droplets so as to obtain the optimal control effect of diseases and pests. The size directly affects the adhesion, slippage or drift of pesticide droplets, which are important indicators to measure the quality of spray [19,20]. Therefore, based on the atomization parameters of VMD and RS, the research on the influence factors and laws of the spatial distribution of the droplet size is of great significance for controlling spray operations, improving the utilization of pesticides and reducing pesticide residues.

In the spray operation, the droplet size is affected by meteorological conditions, pesticide characteristics, spray parameters, spatial parameters and so on [21–24]. In order to precisely control the spatial distribution of droplet size, it is necessary to study the correlation between different influence factors and droplet size. Among them, spray parameters and spatial parameters are easy to control during the operation. Therefore, many researchers focus on the analysis of these parameters. The nozzle type and the flow rate are the focus of attention in spray parameters. The nozzle is the main component to atomize the sprayed liquid, and its type and structure directly determine the characteristics of the droplet spectrum [25]. Kang et al. [26] obtained atomization models of different nozzles, which was validated by actual test method and showed a high degree of confidence. Kooij et al. [27] studied the liquid film generated by nozzles of different shapes. In many studies, the droplet size distribution between different nozzles was compared [25,28,29]. In order to improve the utilization rate of pesticides, low-volume spray mode is widely used [30,31]. The spraying flow rate also becomes an important parameter in the spraying operation. A suitable droplet size distribution can be achieved with the proper selection of the nozzle and the flow rate. Balsari et al. [32] measured droplet size parameters and RS in different combinations between flow rates and air speed. The spatial parameters refer to the spray height and the horizontal distance between the target crop and the nozzle. Studies have shown that there are significant differences in the droplet size distribution at different locations [8,33]. During the unmanned aerial vehicle (UAV) spraying operation, the flying height directly affects the droplet deposition effect [34]. The droplet deposition effects at different horizontal positions are also different, which is an important factor in determining the nozzle position and the horizontal distance between the two flight routes [35]. In variable spraying process, the uniformity of droplet deposition is often improved by adjusting the spatial parameters [36]. In summary, the spray parameters and spatial parameters should be considered comprehensively to achieve a better spraying effect.

Most of the current studies only focus on single or dual factors when establishing analysis models without comprehensive consideration of spray parameters and spatial parameters. In order to guide spraying operations, it is necessary to establish a prediction model of droplet size distribution considering multiple factors. In addition, polynomial regression models were mainly used, of which the accuracy needs to be improved (determination coefficients were all less than 0.85) [8,32,33]. Machine learning is an important research field of artificial intelligence, which can be used to mine the potential laws behind data and achieve effective use of data through independent learning. Its basic principle is to build a model according to the effective information provided by the calibration set, and then realize the prediction of the newly input sample information. During the

plant protection spray, the droplet size distribution is affected by many factors, which also interact with each other. The influences of spray parameters and spatial parameters on droplet size are different and nonlinear, so the polynomial regression has a poor fitting effect. In this case, the machine learning methods can transform the problem from low-dimensional nonlinearity to high-dimensional linearity, thereby making the prediction results better. Among them, multi-layer perceptron (MLP) can effectively self-learn the interaction between factors while extreme learning machine (ELM) has a fast learning speed. Decision tree (DT), support vector regression (SVR) and radial basis function neural network (RBFNN) have a strong ability to deal with nonlinear issues. These methods combined with spectral technology have achieved good results in detection of crop diseases [37], determination of crop origins [38,39] and prediction of physiological indexes [40,41]. It confirms the superiority of machine learning in mining the relationship between variables. However, as far as we know, machine learning methods have not been widely used in quantitative analysis of droplet size distribution of plant protection spray. Therefore, the main purpose of this study is to investigate the influence of multiple factors on the droplet size distribution as well as the establishment of prediction model based on machine learning. Specifically, that is to (1) investigate the effects of nozzle orifice diameter, flow rate, spray height, horizontal position on VMD and RS; (2) establish quantitative prediction models of VMD and RS, and explore the feasibility of machine learning methods to predict the droplet size distribution; (3) realize the visualization distribution of VMD and RS based on the optimal prediction model. According to the results of the droplet size distribution and the optimal droplet size for the target, the optimal spray parameters and spatial parameters can be determined to realize the uniform distribution of pesticide deposition and exert the best effect of pesticides.

2. Materials and Methods

2.1. Experimental Instrument

The droplet size test system consists of a spray system (including spray controller, nozzle, pump, flowmeter and water tank), a laser particle size analyzer, a moveable bracket and a computer (Figure 1). The test nozzles were hollow cone nozzles of TR80 series (Lechler GmbH, Metzingen, Germany), of which the details were shown in Table 1. In this experiment, the nozzle was fixed on a sliding block which was mounted on the movable bracket to change the position of the nozzle. The bracket is adjustable in height, which ranges from 1 m to 3 m. The PW180-B laser particle size analyzer (Shandong Naikete Analytical Instrument Co., Ltd., Jinan, China) was used to measure the droplet size to evaluate the spray characteristics under different conditions. The measurement range of particle size of the laser particle size analyzer is 1–1000 μm and the repeatability error is within 1%. The spray liquid was water.

Table 1. Information of hollow-cone nozzles.

Nozzle Types	Diameter of Nozzle Orifice (mm)	Flow Rates (L/min)
TR8001	1.0	0.4, 0.5, 0.6
TR80015	1.2	0.5, 0.6, 0.7
TR8002	1.4	0.6, 0.8, 1.0
TR8003	1.8	0.8, 1.0, 1.2

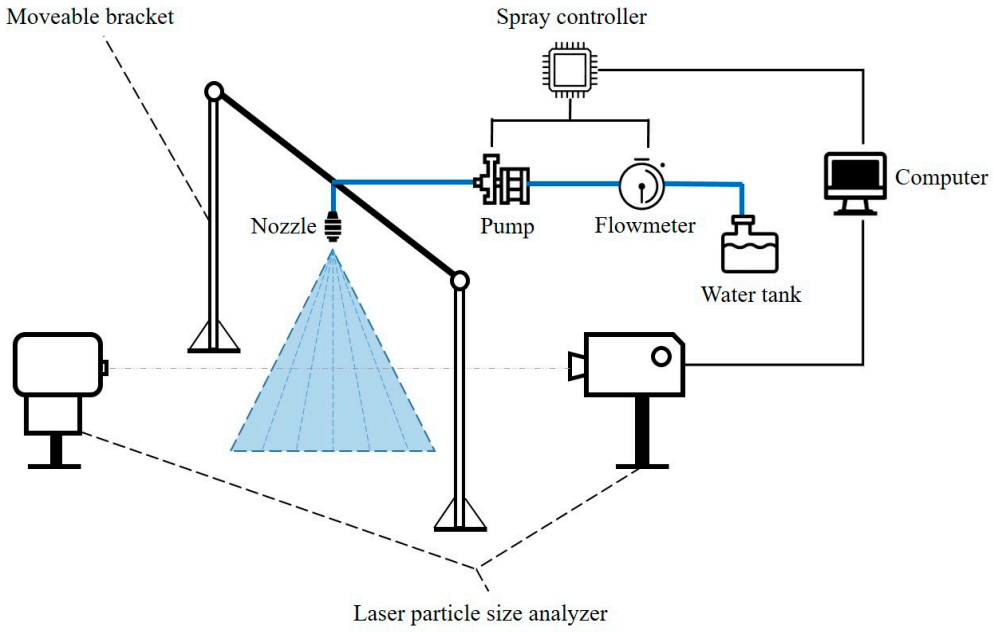


Figure 1. Arrangement of experimental instrument.

2.2. Experimental Method

The test was carried out indoors under windless condition. The temperature was 27 ± 2 °C and the humidity was 60 ± 5%. Three flow modes were selected for each nozzle in the test. According to the commonly used height of UAV spraying, three spray heights were selected, which were 0.50 m, 0.75 m and 1.00 m, respectively. As shown in Figure 2, the point on the spray fan centerline was taken as the origin for each height level and the test points were distributed to both sides of the origin. The distance between two adjacent test points was 50 mm. When measuring, the test point gradually moved away from the centerline to the edge of the spray fan, so as to obtain the horizontal distribution of the droplet size on a certain height. In order to ensure the stability of measurement, the droplet size was measured once the spray situation was stable (the data of the droplet size was stable for about 10 s). For each spray situation, three nozzles of each type were tested and the measurement was repeated 10 times for each nozzle.

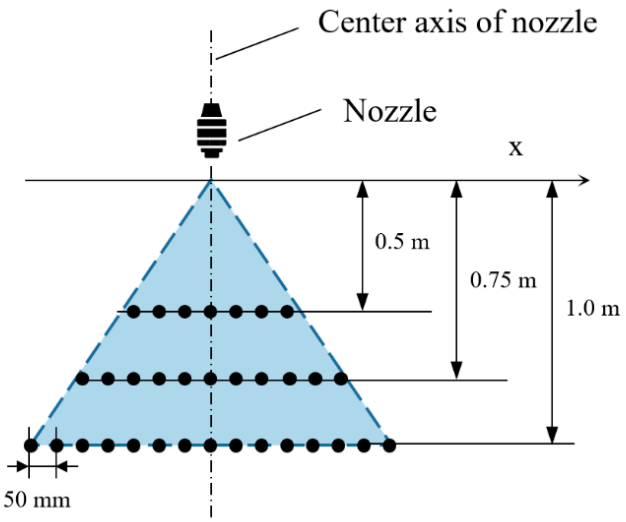


Figure 2. Distribution of particle size test points.

2.3. Performance Evaluation

According to the American Society of Agricultural and Biological Engineers (ASABE) and the American National Standards Institute (ANSI) 572.1 standards [42], VMD and RS of droplets were chosen as the atomization parameters to evaluate the droplet size distribution in this paper [9,20]. VMD is the droplet diameter such that 50% of the spray liquid volume consists of droplets smaller than that value. VMD can reflect the size of the droplet group and serve as the basis for nozzle selection. RS describes the uniformity of droplet size distribution. It is calculated by the following equation:

$$RS = \frac{D_{90} - D_{10}}{VMD} \quad (1)$$

where D_{90} and D_{10} are the respective droplet diameter such that 10% and 90% of the spray liquid volume consists of droplets smaller than that value. The smaller the RS is, the narrower the droplet size spectrum is, indicating that the uniformity of the droplet size distribution is better.

Correlation coefficient (R) and root mean squared error (RMSE) were evaluation indexes for quantitative analysis model in this paper. R can describe the fitting effect of the model, which is better when R is close to 1. R_c and R_p represent the correlation coefficient of the calibration set and prediction set, respectively. The calculation formula of R is as follows:

$$R = \frac{\sum_{i=1}^{N} (\hat{y}_i - \overline{\hat{y}})(y_i - \overline{y})}{\sqrt{\sum_{i=1}^{N} (\hat{y}_i - \overline{\hat{y}})^2 (y_i - \overline{y})^2}} \quad (2)$$

where y_i and $\hat{y}_i$ are the measured and predicted values of the i-th sample, respectively; $\overline{y}$ and $\overline{\hat{y}}$ are the average values of measured and predicted values, respectively; N is the number of samples.

RMSE is used to describe the prediction error of model, which is better when close to zero. Root mean squared error of calibration (RMSEC) and prediction (RMSEP) represent RMSE of the calibration set and prediction set, respectively. It is calculated by the following equation:

$$RMSE = \sqrt{\frac{1}{N-1} \cdot \sum_{i=1}^{N} (y_i - \hat{y}_i)^2} \quad (3)$$

where y_i and $\hat{y}_i$ are the measured value and the predicted value of the i-th sample, respectively; N is the number of samples.

2.4. Data Treatment

In this paper, the data analysis was performed on Matlab R2014a (the MathWorks Corporation, Natick, MA, USA), Anaconda3 (Anaconda, Inc., Austin, TX, USA) and SPSS 16.0 (International Business Machines Corporation, Armonk, NY, USA). One-way ANOVA was used to analyze the influence of different factors on atomization parameters. The significant difference was evaluated according to the Duncan's test ($\alpha = 0.05$).

Moreover, quantitative analysis models of VMD and RS were established through polynomial regression and machine learning methods, where MLP, DT, SVR, ELM and RBFNN were chosen. Polynomial regression is a form of linear regression which is widely used because of its flexibility. Its modelling effects were compared with those of the machine learning methods in this paper. MLP is a back-propagation algorithm with autonomous learning capabilities, which is currently the most widely used multilayer feed forward neural network [43]. Each neuron in its hidden layer has a nonlinear activation function, and the number of neurons directly affects the results of the model. By comparing the output value with the actual value, the network connection weight is optimized from back to front until the network tends to be stable. DT is a common machine learning method which represents a mapping between object attributes and object values. Each internal node represents the judgment condition and its branch represents objects that meet the condition

while the leaf node of the tree represents the prediction result. DT is suitable for processing high-dimensional data, which has advantages of fast speed and high training accuracy [44]. SVR is a supervised modeling method, which can effectively perform regression of high-dimensional data sets. It maps input data from the low-dimensional feature space to a high-dimensional feature space by the kernel function. Then the optimal hyperplane is sought to minimize the total deviation of all samples [45,46]. ELM is a single-hidden layer feed forward neural network. The input weight and hidden layer bias are set as random and unchanged so that the matrix of output weights can be determined. Compared with the traditional neural networks, ELM can learn faster with better generalization performance while ensuring learning accuracy [47]. RBFNN is a feed forward neural network with an input layer, a hidden layer, and an output layer. The input data is mapped directly to a higher-dimensional space through radial basis functions of the neurons in the hidden layer. The prediction result is obtained through the linear weighted sum of outputs of hidden layer neurons. RBFNN learns faster than the back propagation neural network [48].

3. Results and Discussion

3.1. Influence of Different Factors on the Droplet Size Distribution

3.1.1. Droplet Size Distribution of Different Nozzle Orifice Diameters

The flow rate of the nozzles TR8001, TR80015 and TR8002 was set as 0.6 L/min while spray heights were set as 0.50 m, 0.75 m and 1.00 m, respectively. Taking the centerline of the spray fan as the measuring position, the influence of nozzle orifice diameters on droplet size distribution was investigated.

The VMD increased significantly as orifice diameters increased (Table 2). There were similar variations at different heights. The VMD ranged from 101.07–179.48 μm, so it could be regarded as fine droplets (101–200 μm), meeting the optimal range of biological droplet size for different control objects [33]. RS decreased with orifice diameters increased (Table 3), indicating more uniform droplet size distribution. The RS of TR8001 was significantly larger than those of the other nozzles while there was no significant difference between TR80015 and TR8002 at the heights of 0.50 m and 0.75 m. However, the RSs were significantly different at height of 1 m. When the flow rate was the same, the initial speed of sprayed liquid from nozzles with small orifice diameter was large, leading to high kinetic energy for fragmentation. As a result, smaller droplets would be atomized and the VMD decreased with the decreasing orifice diameter [49]. RS decreased with the increase of droplet size, indicating that the uniformity of droplet size distribution got better.

Table 2. Effect of the orifice diameters on VMD (μm).

Nozzle Types	Orifice Diameter (mm)	Height (m)		
		0.50	**0.75**	**1.00**
TR8001	1.0	101.07 ± 1.91 ^{c}	105.66 ± 2.49 ^{c}	104.74 ± 2.63 ^{c}
TR80015	1.2	118.42 ± 2.49 ^{b}	134.21 ± 4.21 ^{b}	135.05 ± 3.4 ^{b}
TR8002	1.4	163.8 ± 2.01 ^{a}	160.31 ± 5.4 ^{a}	179.48 ± 4.35 ^{a}

Note: values are means ± SD. Values in the same column followed by different lowercase letters are significantly different (Duncan's test $p < 0.05$).

Table 3. Effect of the orifice diameters on RS.

Nozzle Types	Orifice Diameter (mm)	Height (m)		
		0.50	**0.75**	**1.00**
TR8001	1.0	1.2794 ± 0.0366 ^{a}	1.3591 ± 0.055 ^{a}	1.4114 ± 0.0236 ^{a}
TR80015	1.2	1.235 ± 0.0357 ^{b}	1.3037 ± 0.0463 ^{b}	1.3597 ± 0.0297 ^{b}
TR8002	1.4	1.2338 ± 0.0263 ^{b}	1.301 ± 0.0612 ^{b}	1.2656 ± 0.0237 ^{c}

Note: values are means ± SD. Values in the same column followed by different lowercase letters are significantly different (Duncan's test $p < 0.05$).

3.1.2. Droplet Size Distribution of Different Flow Rates

Taking TR80015 as an example, the flow rate was set as 0.5 L/min, 0.6 L/min and 0.7 L/min, respectively, while the spray heights were 0.50 m, 0.75 m and 1.00 m, respectively. Taking the centerline of the spray fan as the measuring position, the influence of flow rates on droplet size distribution was investigated.

As shown in Table 4, VMD decreased with the increasing flow rates. When the spray height was 0.50 m and 0.75 m, there was a significant difference between VMDs at different flow rates. When the spray height was 1.00 m, the VMD at flow rate of 0.5 L/min was significantly higher than those at other flow rates, and there was no significant difference between the VMDs at flow rate of 0.6 L/min and 0.7 L/min. The initial speed of sprayed liquid was larger as flow rate increased, leading to the high kinetic energy for fragmentation. As a result, the VMD decreased.

Table 4. Effect of the flow rates on VMD (μm).

Flow Rate (L/min)	Height (m)		
	0.50	**0.75**	**1.00**
0.5	138.19 ± 1.76 ^{a}	147.67 ± 2.16 ^{a}	153.32 ± 3.21 ^{a}
0.6	118.42 ± 2.49 ^{b}	134.21 ± 4.21 ^{b}	135.05 ± 3.4 ^{b}
0.7	114.13 ± 2.52 ^{c}	126.53 ± 3.53 ^{c}	134.75 ± 4.52 ^{b}

Note: values are means ± SD. Values in the same column followed by different lowercase letters are significantly different (Duncan's test $p < 0.05$).

As shown in Table 5, when the spray height was 0.5 m, the RS at flow rate of 0.7 L/min was significantly higher than those at other flow rates. Besides, there was no significant difference between the RSs at flow rates of 0.5 L/min and 0.6 L/min. When the spray height was 0.75 m, RS showed a significant increasing trend with the increasing flow rates. When the spray height was 1.00 m, the RS at flow rate of 0.5 L/min was the lowest while there was no significant difference between the RSs at flow rates of 0.6 L/min and 0.7 L/min.

Table 5. Effect of the flow rates on RS.

Flow Rate (L/min)	Height (m)		
	0.50	**0.75**	**1.00**
0.5	1.248 ± 0.0374 ^{b}	1.2633 ± 0.0289 ^{c}	1.2459 ± 0.0381 ^{b}
0.6	1.235 ± 0.0357 ^{b}	1.3037 ± 0.0463 ^{b}	1.3597 ± 0.0297 ^{a}
0.7	1.3127 ± 0.025 ^{a}	1.3541 ± 0.0437 ^{a}	1.3358 ± 0.0629 ^{a}

Note: values are means ± SD. Values in the same column followed by different lowercase letters are significantly different (Duncan's test $p < 0.05$).

3.1.3. Droplet Size Distribution of Different Spatial Positions

Taking TR80015 nozzle as an example, the droplet size distribution at different spatial positions was investigated with a flow rate of 0.6 L/min. The results were shown in Figure 3, and the significance analysis was listed in Tables S1 and S2 (Supplementary Materials).

Generally speaking, VMD increased significantly with the rise of height and the increase of horizontal distance from the centerline. It could be seen from Figure 3a that the spatial variation curves of VMD were approximately symmetrically distributed with the centerline of the spray fan as the axis, showing the shape of 'V' [50]. There was no significant difference between VMDs of two test points that were at the same horizontal distance from the centerline. The VMD at the origin was the smallest while that at the edge of the spray fan was the largest. The influence of horizontal position on VMD was consistent at different spray heights. Furthermore, the growth rate of VMD increased at the beginning and then slowed down as the horizontal distance increased.

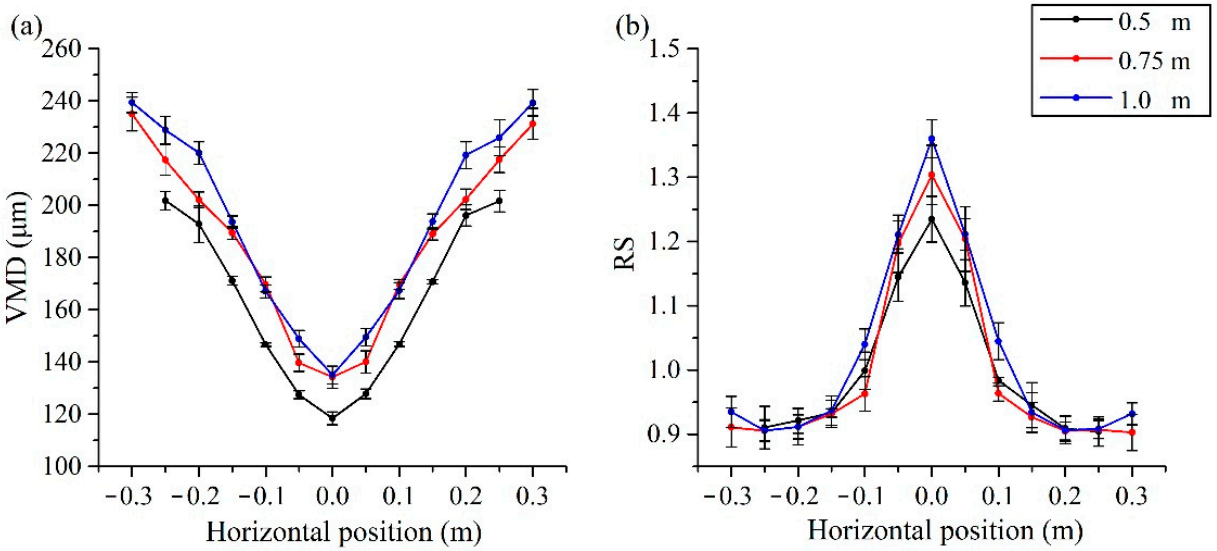


Figure 3. Droplet size distribution at different spatial positions: (**a**) VMD; (**b**) RS.

In Figure 3b, the spatial variation curves of RS were symmetrically distributed around the centerline of the spray fan, showing a convex shape. There was no significant difference between RSs of two test points which were at the same horizontal distance from the centerline. When the distance from the centerline was within 0.15 m, RS decreased rapidly with the distance increased, indicating better uniformity of droplet size distribution. Besides, the RSs at different heights showed significant difference and tended to rise with increasing heights. When the distance ranged from 0.15 m to the edge, the RS stabilized and showed no significant difference at the heights of 0.5 m and 0.75 m while the RS at the height of 1.00 m had a slow decline followed by a slight rise as the distance increased. Furthermore, there was no significant difference between RSs of different heights at the same horizontal position.

On one hand, during the process of downward transportation of droplets, small droplets converged towards the central area due to the entrainment effect caused by the speed difference of the surrounding airflow. The larger droplet was less affected by the entrainment effect for its large initial kinetic energy, so it had a strong diffusion ability to reach the edge of the spray fan. In addition, the probability of small droplets combining with other droplets to form larger droplets increased as the movement distance increased. Therefore, the VMD in the middle of the spray fan was the smallest. On the other hand, the velocity of the droplets gradually attenuated due to the effect of air resistance, which weakened the entrainment effect. Moreover, the speed of the small droplets decayed faster. As a result, part of small droplets lost their kinetic energy and floated in the air before reaching the test point [51,52]. Therefore, the droplet size increased significantly with the increase of height and horizontal distance.

3.2. Quantitative Model of Atomization Parameter

Spray is a complex physical process, in which the influence the combination of spray and spatial parameters on the droplet size distribution is non-linear. The atomization effect of the nozzle is the key to the control effect. Therefore, quantitative evaluation models for predicting VMD and RS were established with nozzle orifice diameter, flow rate, spray height and horizontal position taken as independent variables. In order to ensure the robustness of model, all data were divided into calibration set and prediction set at a ratio of 3:1, of which the details were shown in Table 6.

Table 6. Statistics on sample set partitioning.

Evaluation Index	Calibration Set			Prediction Set		
	Range	Average	SD	Range	Average	SD
VMD (μm)	101.07–322.58	196.29	48.00	104.74–307.91	196.58	50.49
RS	0.8738–1.4313	1.0164	0.1318	0.8675–1.4114	1.0164	0.1315

3.2.1. VMD Quantitative Prediction Model

The quantitative models for VMD were established based on polynomial regression, DT, MLP, RBFNN, ELM and SVR methods, respectively (Table 7 and Figure 4). All models achieved excellent results in predicting VMD, of which R_c and R_p reached 0.95. Polynomial regression is currently the most commonly used method to fit the relationship between VMD and spray parameters. However, the error of polynomial regression model was relatively large, of which the RMSEC and RMSEP were 13.5316 μm and 15.3068 μm, respectively. Compared with other methods, the prediction effect was poor. The VMD prediction scatter plot of each model was shown in Figure 4. It could be seen from Figure 4b that the calibration set of the DT model had a better fitting effect while the prediction set had a larger deviation, indicating poor stability. In addition, both the MLP model and the RBFNN model had good fitting results, of which R_c and R_p were above 0.98. It was worth noting that the fitting results of the ELM model and the SVR model were relatively close, and the R_c and R_p were both above 0.99. The R_c and R_p of the SVR model were 0.9974 and 0.9929, respectively, while the RMSEC and RMSEP were 3.4790 μm and 6.0690 μm, respectively. Compared with the other five models, the SVR model had higher R_p and smaller RMSE, which proved that this method was more suitable for predicting VMD.

Table 7. Model parameters of different models in predicting VMD.

Model	Parameter [a]
Polynomial regression	2
DT	11
MLP	10, 5
RBFNN	1.69
ELM	162
SVR	1000, 10

[a] Parameters of different models: the highest power for polynomial regression, the maximum depth for DT, the number of neurons in each hidden layer for MLP, the spread coefficient for RBFNN, the number of neurons in hidden layer for ELM, the penalty coefficient (C) and RBF function parameters (Gamma) for SVR.

3.2.2. RS Quantitative Prediction Model

Similarly, quantitative models for RS were established based on polynomial regression, DT, MLP, RBFNN, ELM and SVR methods (Table 8 and Figure 5). The R_p and RMSEP of polynomial regression were 0.5989 and 0.1055, respectively, indicating that the model had poor fitting effect with large prediction errors. In addition, although the SVR method achieved good results in establishing the VMD evaluation model, the effect in predicting RS was not ideal and the R were less than 0.9. As for RBFNN, ELM, DT models, good results were achieved in calibration while the prediction errors of these models were relatively large. It could be seen from Figure 5c–e that the scatter points of prediction set deviated from the fitting curve more obviously, which indicated that these models were not appropriate to predict RS. Although the R_c and R_p of DT model were both greater than 0.9, the sensitivity of this method to variables was poor. When the spray parameter was within a certain range, the predicted RS value was constant while the actual value changed in real time, so the applicability of DT model was poor. Compared with the other five models, MLP achieved the best modeling result, of which the R_p and RMSEP were 0.9537 and 0.0398, respectively. Therefore, MLP model was more suitable for predicting RS.

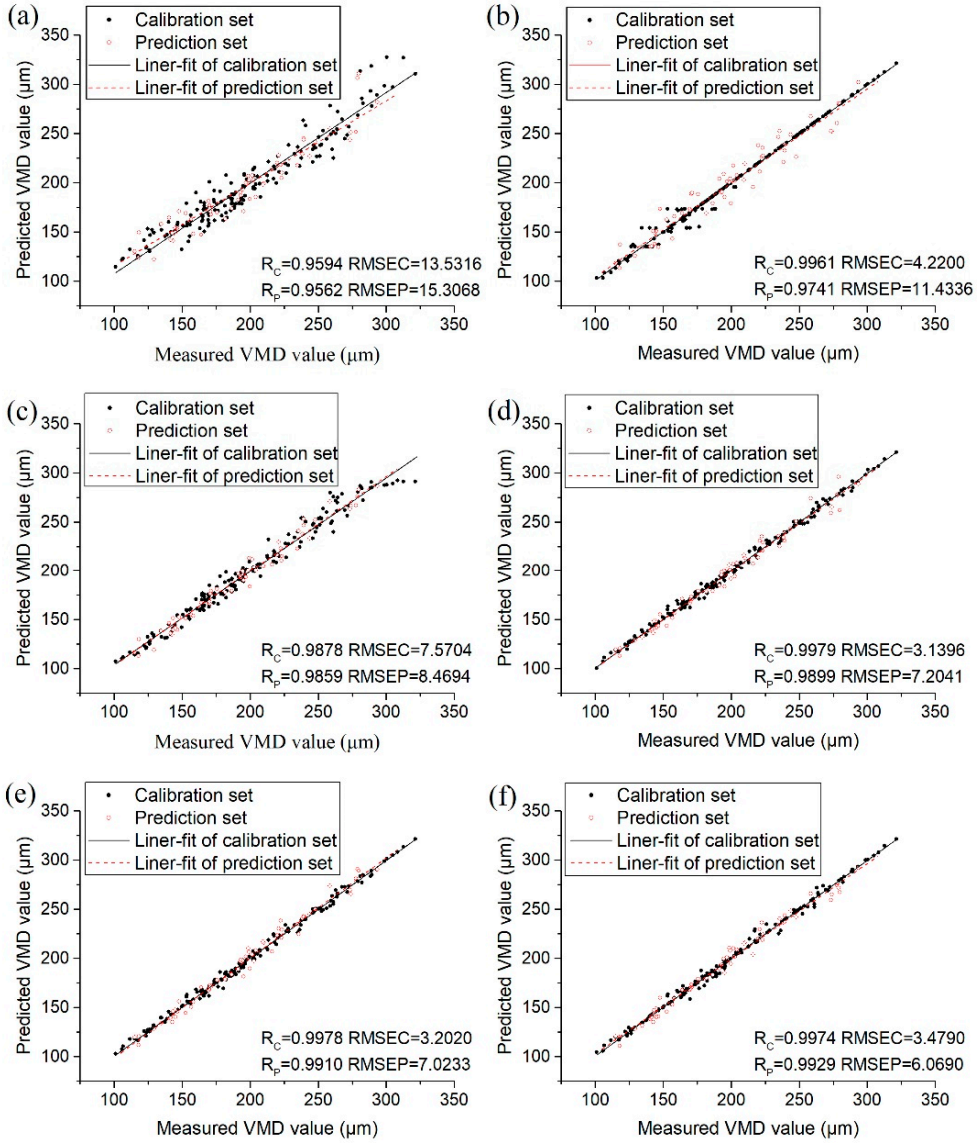


Figure 4. Scatter plot of measured value and predicted value of VMD: (**a**) polynomial regression; (**b**) DT; (**c**) MLP; (**d**) RBFNN; (**e**) ELM; (**f**) SVR.

Table 8. Model parameters of different models in predicting RS.

Model	Parameter [a]
Polynomial regression	2
SVR	1000, 6.173
RBFNN	2.06
ELM	148
DT	5
MLP	10, 5

[a] Parameters of different models: the highest power for polynomial regression, the penalty coefficient (C) and RBF function parameters (Gamma) for SVR, the spread coefficient for RBFNN, the number of neurons in hidden layer for ELM, the maximum depth for DT, the number of neurons in each hidden layer for MLP.

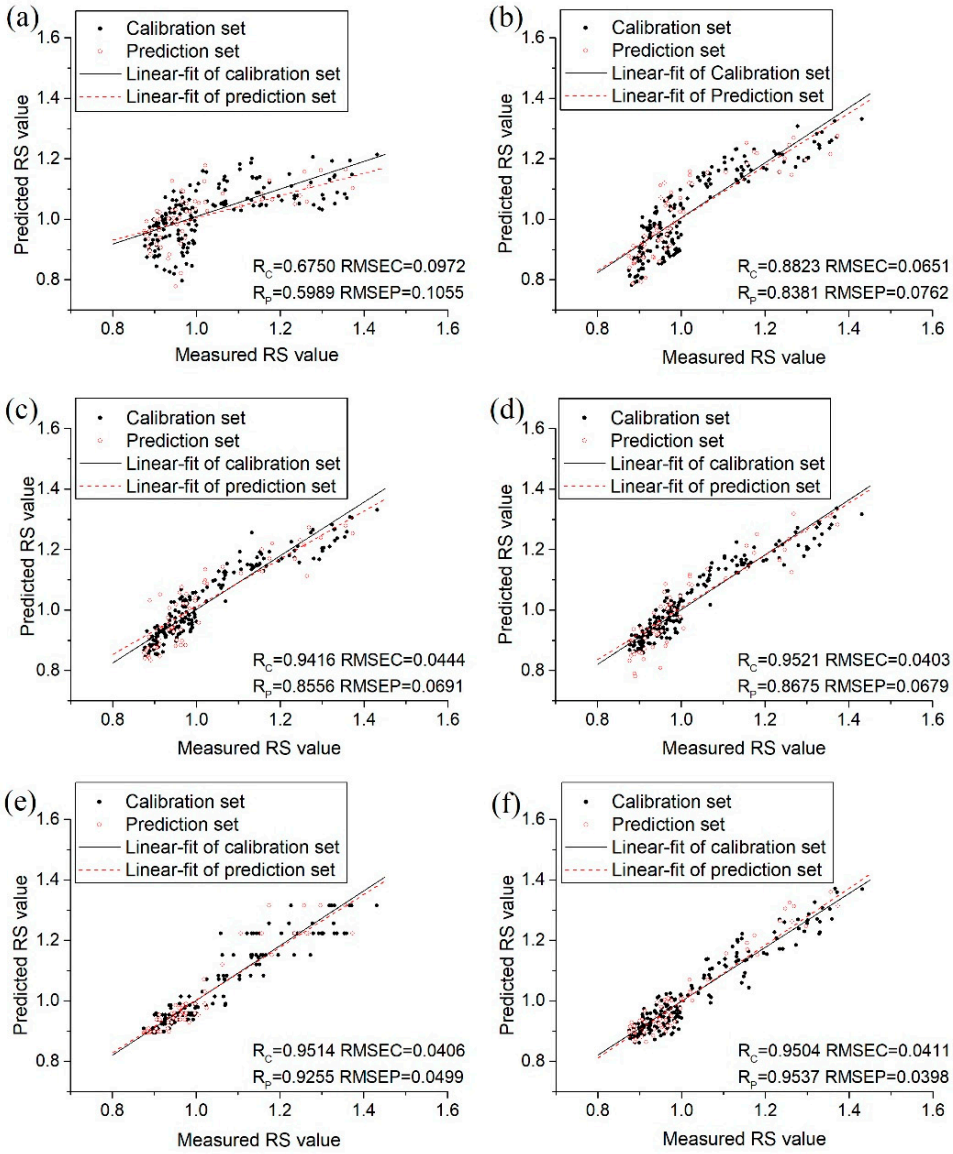


Figure 5. Scatter plot of measured value and predicted value of RS: (**a**) polynomial regression; (**b**) SVR; (**c**) RBFNN; (**d**) ELM; (**e**) DT; (**f**) MLP.

3.2.3. Visualization of Droplet Size Distribution

The spatial distribution of droplet size measured by instrument is usually discrete. In order to provide guidance for the agricultural spray operation, it is necessary to understand the spatial continuous distribution of atomization parameters. Therefore, the spatial distribution visualization of VMD and RS was realized by using the established quantitative models. Taking TR80015 nozzle with flow rate of 0.6 L/min as an example, SVR and MLP were chosen on account of their excellent performance to predict the distribution of VMD and RS, respectively. Moreover, the pseudo-color processing was carried out on the image to obtain the spatial continuous distribution of VMD and RS (Figures 6 and 7).

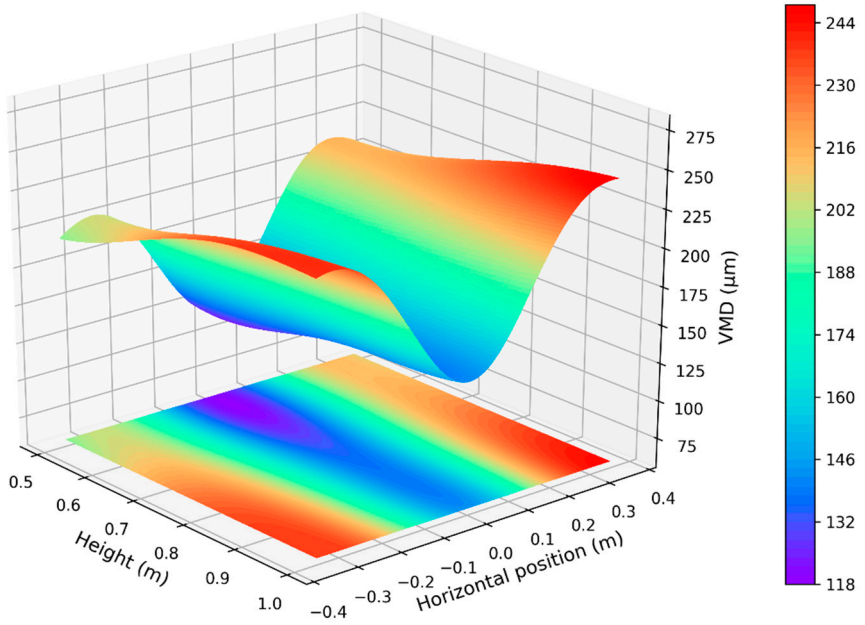


Figure 6. Visualization of VMD distribution.

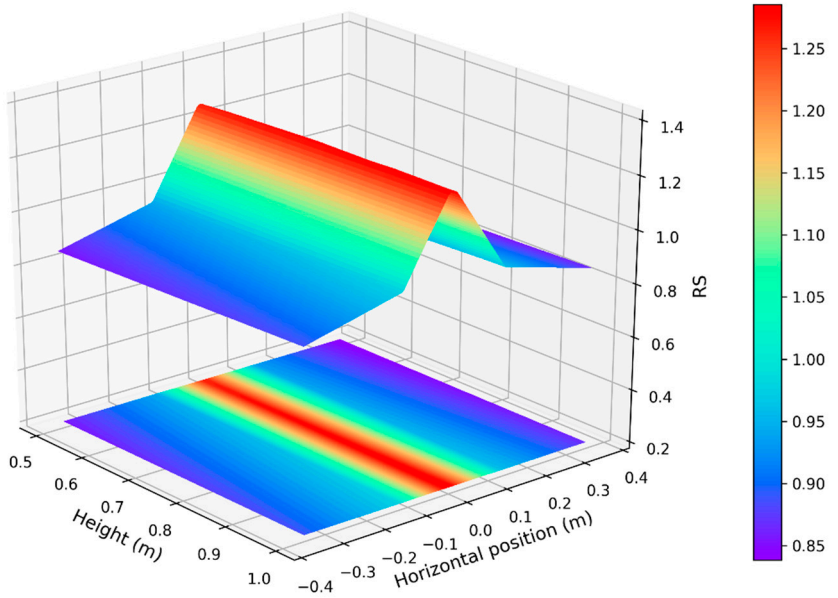


Figure 7. Visualization of RS distribution.

The spatial distribution of VMD and RS conformed to the description in Section 3.1.3. It could be seen from Figures 6 and 7 that, the changes of VMD and RS were more obvious with the increase of the horizontal position and thus the influence of the horizontal position on the atomization parameters was greater than spray height. Only part of large droplets could reach the edge of spray fan, leading to a large VMD and uniform droplet size distribution (small RS). When the horizontal distance was further extended, the amount of droplets reduced rapidly and the small droplets that floated in the air might appear in this position, accounting for the situation that there was a slight decrease of VMD. The trend of RS was opposite to that of VMD. Moreover, there was an obvious turning point when the horizontal distance was between 0.1 m and 0.15 m where the reduction rate of RS suddenly became small.

No matter whether the vehicle is the land machinery or unmanned aerial vehicle, the cooperation of multiple nozzles is often applied in the spray operation. In order to ensure

uniform application of pesticides at all positions in the horizontal direction, the nozzles are mounted on the spray rod at certain intervals [53]. The installation position of nozzles and the horizontal angle between the nozzle and the spray rod should be reasonably arranged after determining the spray parameters and droplet size distribution, so as to achieve better prevention and control effect. An accurate prediction model of droplet size distribution is an important basis for optimization of nozzle installation parameters. In summary, visualization analysis based on the optimal prediction model can display the spatial distribution information of VMD and RS, which helps to determine the spray parameters and spatial parameters required for the optimal droplet size.

4. Conclusions

The quantitative analysis of droplet size distribution is crucial to the effectiveness of spray operations. In this research, VMD and RS were selected as the atomization indexes to evaluate the distribution of droplet size. The influence of nozzle orifice diameter, flow rate, spray height and horizontal position on the spatial distribution of droplet size was investigated. In addition, quantitative evaluation models were established for predicting RS and VMD based on machine learning methods. The specific conclusions are as follows: (1) as the orifice diameter increased or flow rate decreased, VMD increased and RS decreased. (2) Spatial parameters (spray height and horizontal position) had an impact on the distribution of droplet size. The variation curves of VMD and RS were approximately symmetrically distributed around the centerline of the spray fan. With the increase of spray height and horizontal distance, VMD showed an increasing trend. There was an obvious turning of RS reduction rate at some horizontal position. RS decreased with the increasing horizontal distance or the decreasing height within this value while the influence of spatial parameters on RS was not obvious when the horizontal distance was larger than this value. (3) The models based on machine learning for predicting VMD all achieved a better result than polynomial regression. Among them, SVR model had the best prediction effect, of which R_p and RMSEP were 0.9929 and 6.0690, respectively. For RS, MLP model achieved a better result in predicting RS, of which R_p and RMSEP were 0.9537 and 0.0398 respectively, while there was overfitting in the other models. Compared with machine learning methods, the polynomial regression model had a large error in predicting RS, and its R_p was only 0.5989.

The results show that machine learning methods have provided a novel and feasible method for quantitative evaluation of droplet size distribution. The accurate prediction model of droplet size distribution provides an important basis for optimizing nozzle installation parameters, and the visualization results based on models can provide intuitive guidance for spray operations. Combining the optimal droplet size of the target crop with the visual distribution, the nozzle parameters and operating parameters, such as the selection of nozzle type, nozzle position arrangement, spray height and flow rate, can be modified in a targeted manner, providing a basis for realizing the uniform distribution of pesticide deposits and further research on droplet distribution during multi-nozzle operation. Therefore, it is very meaningful to apply the prediction model based on machine learning to the variable spraying system for prediction of droplet size distribution.

Supplementary Materials: The following are available online at https://www.mdpi.com/article/10.3390/w14020175/s1, Table S1: Effect of spatial positions on VMD (μm), Table S2. Effect of spatial positions on RS.

Author Contributions: Conceptualization, Y.H.; Data curation, J.W.; Formal analysis, J.W.; Funding acquisition, H.F.(Hui Fang); Investigation, J.W. and H.F.(Haoluan Fu); Methodology, Y.H.; Project administration, Y.H.; Resources, H.F.(Hui Fang); Software, J.W. and H.F.(Haoluan Fu); Supervision, Y.H.; Validation, Z.S.; Writing—original draft, J.W.; Writing—review and editing, Y.H., Z.S. and W.W. All authors have read and agreed to the published version of the manuscript.

Funding: This research was funded by (1) National Natural Science Foundation of China, grant number 31801257; (2) Zhejiang Public Welfare Technology Research Program, grant number LGN19F020001; (3) National Key Research and Development Program of China, grant number 2016YFD0200701.

Institutional Review Board Statement: Not applicable.

Informed Consent Statement: Not applicable.

Data Availability Statement: The data used in this study are available from the corresponding author upon request.

Conflicts of Interest: The authors declare no conflict of interest.

References

1. Torrent, X.; Gregorio, E.; Rosell-Polo, J.R.; Arnó, J.; Peris, M.; Van De Zande, J.C.; Planas, S. Determination of spray drift and buffer zones in 3D crops using the ISO standard and new LiDAR methodologies. *Sci. Total Environ.* **2020**, *714*, 136666. [CrossRef]
2. Gil, Y.; Sinfort, C.; Brunet, Y.; Polveche, V.; Bonicelli, B. Atmospheric loss of pesticides above an artificial vineyard during air-assisted spraying. *Atmos. Environ.* **2007**, *41*, 2945–2957. [CrossRef]
3. Yusà, V.; Coscollà, C.; Millet, M. New screening approach for risk assessment of pesticides in ambient air. *Atmos. Environ.* **2014**, *96*, 322–330. [CrossRef]
4. Kira, O.; Linker, R.; Dubowski, Y. Estimating drift of airborne pesticides during orchard spraying using active Open Path FTIR. *Atmos. Environ.* **2016**, *142*, 264–270. [CrossRef]
5. Wang, G.; Lan, Y.; Qi, H.; Chen, P.; Hewitt, A.; Han, Y. Field evaluation of an unmanned aerial vehicle (UAV) sprayer: Effect of spray volume on deposition and the control of pests and disease in wheat. *Pest Manag. Sci.* **2019**, *75*, 1546–1555. [CrossRef]
6. Ebert, T.A.; Downer, R.A. A different look at experiments on pesticide distribution. *Crop Prot.* **2006**, *25*, 299–309. [CrossRef]
7. Yang, F.; Xue, X.; Cai, C.; Zhou, Q.; Sun, Z. Atomization performance test and influence factors of aviation special centrifugal nozzle. *Trans. Chin. Soc. Agric. Mach.* **2019**, *50*, 96–104.
8. Wang, S.; He, X.; Song, J.; Zhang, L.; Dorr Gary, J.; Andreas, H. Measurement comparison and fitted distribution equation of droplet size for agricultural nozzles. *Trans. Chin. Soc. Agric. Eng.* **2014**, *30*, 34–42.
9. Yuan, H.; Wang, G. Effects of droplet size and deposition density on field efficacy of pesticides. *Plant Prot.* **2015**, *41*, 9–16.
10. Wang, G.; Han, Y.; Li, X.; Andaloro, J.; Chen, P.; Hoffmann, W.C.; Han, X.; Chen, S.; Lan, Y. Field evaluation of spray drift and environmental impact using an agricultural unmanned aerial vehicle (UAV) sprayer. *Sci. Total Environ.* **2020**, *737*, 139793. [CrossRef]
11. Torrent, X.; Gregorio, E.; Douzals, J.-P.; Tinet, C.; Rosell-Polo, J.R.; Planas, S. Assessment of spray drift potential reduction for hollow-cone nozzles: Part 1. Classification using indirect methods. *Sci. Total Environ.* **2019**, *692*, 1322–1333. [CrossRef] [PubMed]
12. Gregorio, E.; Torrent, X.; Planas, S.; Rosell-Polo, J.R. Assessment of spray drift potential reduction for hollow-cone nozzles: Part 2. LiDAR technique. *Sci. Total Environ.* **2019**, *687*, 967–977. [CrossRef] [PubMed]
13. Chen, J.; Zhang, D.; He, Z.; Liu, J. Effect of three herbicides on the content of Malondialdehyde and Proline in cotton leaves. *J. Shihezi Univ. (Nat. Sci.)* **2012**, *30*, 33–36.
14. Himel, C.M. The optimum size for insecticide spray droplets2. *J. Econ. Entomol.* **1969**, *62*, 919–925. [CrossRef]
15. Himel, C.M.; Moore, A.D. Spray droplet size in the control of spruce budworm, boll weevil, bollworm, and cabbage looper1. *J. Econ. Entomol.* **1969**, *62*, 916–918. [CrossRef]
16. Himel, C.M.; Uk, S. Dose-toxicity of chlorpyrifos and endosulfan insecticides on house-fly diptera-muscidae by topical, vapor, and spray treatments as estimated by gas-chromatography. *J. Econ. Entomol.* **1972**, *65*, 990–994. [CrossRef] [PubMed]
17. Hewitt, A.J.; Meganasa, T. Droplet distribution densities of a pyrethroid insecticide within grass and maize canopies for the control of spodoptera-exempta larvae. *Crop Prot.* **1993**, *12*, 59–62. [CrossRef]
18. Washington, J.R. Relationship between the spray droplet density of two protectant fungicides and the germination of Mycosphaerella fijiensis ascospores on banana leaf surfaces. *Pestic. Sci.* **1997**, *50*, 233–239. [CrossRef]
19. Peñaloza, E.A.G.; Mercaldi, H.V.; Oliveira, V.A.; Cruvinel, P.E. An Advanced Model Based on Analytical and Computational Procedures for the Evaluation of Spraying Processes in Agriculture. In Proceedings of the IEEE Tenth International Conference on Semantic Computing (ICSC), Laguna Hills, CA, USA, 4–6 February 2016; pp. 432–436.
20. Lan, Y.; Peng, J.; Jin, J. Research status and development of pesticide spraying droplet size. *J. South China Agric. Univ.* **2016**, *37*, 1–9.
21. Santangelo, P.E. Characterization of high-pressure water-mist sprays: Experimental analysis of droplet size and dispersion. *Exp. Therm. Fluid Sci.* **2010**, *34*, 1353–1366. [CrossRef]
22. Mandato, S.; Rondet, E.; Delaplace, G.; Barkouti, A.; Galet, L.; Accart, P.; Ruiz, T.; Cuq, B. Liquids' atomization with two different nozzles: Modeling of the effects of some processing and formulation conditions by dimensional analysis. *Powder Technol.* **2012**, *224*, 323–330. [CrossRef]
23. Zeng, A.; Wang, C.; Song, J.; Wang, Z.; Huang, M.; He, X.; Andreas, H. Effects of nozzle types, adjuvants and environmental conditions on spray drift potential of unmanned aerial vehicles in a wind tunnel. *Chin. J. Pestic. Sci.* **2020**, *22*, 315–323.

24. McGinty, J.; Baumann, P.; Hoffmann, W.; Fritz, B. Evaluation of the spray droplet size spectra of drift-reducing agricultural spray nozzle designs. *Am. J. Exp. Agric.* **2016**, *11*, 1–5. [CrossRef]
25. Ferguson, J.C.; O'Donnell, C.C.; Chauhan, B.S.; Adkins, S.W.; Kruger, G.R.; Wang, R.; Urach Ferreira, P.H.; Hewitt, A.J. Determining the uniformity and consistency of droplet size across spray drift reducing nozzles in a wind tunnel. *Crop Prot.* **2015**, *76*, 1–6. [CrossRef]
26. Kang, F.; Wang, Y.; Li, S.; Jia, Y.; Li, W.; Zhang, R.; Zheng, Y. Establishment of a static nozzle atomization model for forest barrier treatment. *Crop Prot.* **2018**, *112*, 201–208. [CrossRef]
27. Kooij, S.; Sijs, R.; Denn, M.M.; Villermaux, E.; Bonn, D. What Determines the Drop Size in Sprays? *Phys. Rev. X* **2018**, *8*, 031019. [CrossRef]
28. Hoffmann, W.C.; Kirk, I.W. Spray deposition and drift from two "medium" nozzles. *Trans. ASAE* **2005**, *48*, 5–11. [CrossRef]
29. Dai, Q.; Hong, T.; Song, S.; Chen, S.; Zhang, C. Test and analysis of droplet uniformity for pipeline constant pressure spray in orchards. *Guangdong Agric. Sci.* **2016**, *43*, 164–171.
30. Martinez-Guanter, J.; Agüera, P.; Agüera, J.; Pérez-Ruiz, M. Spray and economics assessment of a UAV-based ultra-low-volume application in olive and citrus orchards. *Precis. Agric.* **2020**, *21*, 226–243. [CrossRef]
31. Liu, Q.; Wei, K.; Yang, L.; Xu, W.; Xue, W. Preparation and application of a thidiazuron·diuron ultra-low-volume spray suitable for plant protection unmanned aerial vehicles. *Sci. Rep.* **2021**, *11*, 4998. [CrossRef]
32. Balsari, P.; Grella, M.; Marucco, P.; Matta, F.; Miranda-Fuentes, A. Assessing the influence of air speed and liquid flow rate on the droplet size and homogeneity in pneumatic spraying. *Pest Manag. Sci.* **2018**, *75*, 366–379. [CrossRef] [PubMed]
33. Hu, G.; Xu, L.; Zhou, H.; Cui, Y. Analysis of multi-factor influence on droplet size distribution of hollow cone nozzle. *J. Nanjing For. Univ. (Nat. Sci. Ed.)* **2014**, *38*, 133–136.
34. Zhang, P.; Deng, L.; Lyu, Q.; He, S.; Yi, S.; Liu, Y.; Yu, Y.; Pan, H. Effects of citrus tree-shape and spraying height of small unmanned aerial vehicle on droplet distribution. *Int. J. Agric. Biol. Eng.* **2016**, *9*, 45–52.
35. Liu, Q.; Lan, Y.; Shan, C.; Mao, Y. The influence of spraying parameters of aerial application on droplet deposition characteristics for apple fields. *J. Agric. Mech. Res.* **2020**, *42*, 173–179.
36. Wen, S.; Zhang, Q.; Yin, X.; Lan, Y.; Zhang, J.; Ge, Y. Design of Plant Protection UAV Variable Spray System Based on Neural Networks. *Sensors* **2019**, *19*, 1112. [CrossRef]
37. Kong, W.; Zhang, C.; Huang, W.; Liu, F.; He, Y. Application of Hyperspectral Imaging to Detect Sclerotinia sclerotiorum on Oilseed Rape Stems. *Sensors* **2018**, *18*, 123. [CrossRef]
38. Hong, Z.; He, Y. Rapid and Nondestructive Discrimination of Geographical Origins of Longjing Tea using Hyperspectral Imaging at Two Spectral Ranges Coupled with Machine Learning Methods. *Appl. Sci.* **2020**, *10*, 1173. [CrossRef]
39. Zhu, S.; Zhou, L.; Gao, P.; Bao, Y.; He, Y.; Feng, L. Near-Infrared Hyperspectral Imaging Combined with Deep Learning to Identify Cotton Seed Varieties. *Molecules* **2019**, *24*, 3268. [CrossRef] [PubMed]
40. Wu, D.; Meng, L.; Yang, L.; Wang, J.; Fu, X.; Du, X.; Li, S.; He, Y.; Huang, L. Feasibility of Laser-Induced Breakdown Spectroscopy and Hyperspectral Imaging for Rapid Detection of Thiophanate-Methyl Residue on Mulberry Fruit. *Int. J. Mol. Sci.* **2019**, *20*, 2017. [CrossRef]
41. Wang, W.; Kong, W.; Shen, T.; Man, Z.; Zhu, W.; He, Y.; Liu, F. Quantitative analysis of cadmium in rice roots based on LIBS and chemometrics methods. *Environ. Sci. Eur.* **2021**, *33*, 37. [CrossRef]
42. American Society of Agricultural and Biological Engineers. Spray nozzle classification by droplet spectra. In *ASABE Standard S572.1*; American Society of Agricultural and Biological Engineers: St. Joseph, MO, USA, 2009.
43. Salehi, M.; Razmara, J.; Lotfi, S. A novel data mining on breast cancer survivability using mlp ensemble learners. *Comput. J.* **2020**, *63*, 435–447. [CrossRef]
44. Wang, Y.; Wu, S.; Yan, D.; Li, F.; Wang, C.; Cheng, M.; Sun, W. Determining and mapping the spatial mismatch between soil and rice cadmium (Cd) pollution based on a decision tree model. *Environ. Pollut.* **2020**, *265*, 115029. [CrossRef]
45. Liu, F.; Ye, L.; Peng, J.; Song, K.; Shen, T.; Zhang, C.; He, Y. Fast detection of copper content in rice by laser-induced breakdown spectroscopy with uni- and multivariate analysis. *Sensors* **2018**, *18*, 705. [CrossRef] [PubMed]
46. Yadav, S.A.; Prasad, R.; Vishwakarma, A.K.; Sharma, J.; Verma, B.; Srivastava, P.K. Optimization of dual-polarized bistatic specular scatterometer for studying microwave scattering response and vegetation growth parameters retrieval of paddy crop using a machine learning algorithm. *Comput. Electron. Agric.* **2020**, *175*, 105592. [CrossRef]
47. Wei, Y.; Huang, H.; Chen, B.; Zheng, B.; Wang, Y. Application of extreme learning machine for predicting chlorophyll-a concentration inartificial upwelling processes. *Math. Probl. Eng.* **2019**, *2019*, 8719387. [CrossRef]
48. Liu, Y.W.; Wu, C.J.; Wang, Y.C. Detection of serial arc fault on low-voltage indoor power lines by using radial basis function neural network. *Int. J. Elec. Power* **2016**, *83*, 149–157. [CrossRef]
49. Zhou, R.; Zhang, H.; Zheng, J.; Zhou, H.; Tang, Y.; Wang, D. Study on parameters of mobile spraying to droplet penetration targeting forestry pest and disease control. *J. Cent. South Univ. For. Technol.* **2019**, *39*, 114–122.
50. Song, J.; Liu, Y.; Zhang, J.; He, X.; Zeng, A.; Herbst, A. Drift mechanism of flat fan nozzle. *Trans. Chin. Soc. Agric. Mach.* **2011**, *42*, 63–69.
51. Jia, W.; Wen, Z.; Yan, M.; Ou, M.; Cheng, Z.; Dong, X. Experimental investigation of droplet characteristics and drift performance in air-assist boom sprayer. *J. Agric. Mech. Res.* **2017**, *39*, 162–167.

52. Zhang, H.; Dorr, G.; Zheng, J.; Zhou, H. Wind tunnel experiment of influence on droplet size distribution of flat fan nozzles. *Trans. Chin. Soc. Agric. Mach.* **2012**, *43*, 53–57.
53. Hilz, E.; Vermeer, A.W.P. Spray drift review: The extent to which a formulation can contribute to spray drift reduction. *Crop Prot.* **2013**, *44*, 75–83. [CrossRef]